Open Access
Baghdad Science Journal **Vol.16(4) 2019**

DOI: http://dx.doi.org/10.21123/bsj.2019.16.4.0910

Studying the Crystal Structure, Topography, and Anti-bacterial of a Novel Titania (TiO_2 NPs) Prepared by a Sol-gel Manner

Ali Abdullah Fayyadh [1*] ***Abbas Fadhel Essa*** [1] ***Shatha Shammon Batros*** [2]
Zinah Shakir Shallal [3]

Received 25/7/2018, Accepted 4/4/2019, Published 1/12/2019

Abstract:

In this research, titanium dioxide nanoparticles (TiO_2 NPs) were prepared through the sol-gel process at an acidic medium (pH3).TiO_2 nanoparticles were prepared from titanium trichloride ($TiCl_3$) as a precursor with Ammonium hydroxide (NH_4OH) with 1:3 ratio at 50 °C. The resulting gel was dried at 70 °C to obtain the Nanocrystalline powder. The powder from the drying process was treated thermally at temperatures 500 °C and 700 °C. The crystalline structure, surface morphology, and particle size were studied by using X-ray diffraction (XRD), Atomic Force Microscopy (AFM), and Scanning Electron Microscope (SEM). The results showed (anatase) phase of titanium dioxide with the average grain size of 110 nm at 500 °C calcination temperature, and (anatase- rutile) mixed phase of titanium dioxide with the average particle size of 118.1 nm at 700 °C calcination temperature. The anti-bacterial activity of the synthesis specimens was recorded through the Kirby-Bauer disc method (disc devotion method). The results displayed a pretty excellent antibacterial activity of TiO_2 NPs to bacteria strains: Gram positive staphylococcus aureus, gram negative pseudomonas aeruginosa, and gram negative escherichia coli. The sensitivity of the tested bacteria to TiO_2 NPs depends on the oxidation state of the TiO_2 NPs, particle size, volume, and the density of the unit cell. The small- average particle size of titanium dioxide particles showed high antibacterial activity against bacteria, while the larger- average particle size of titanium dioxide particles showed less antibacterial activity. The novelty of this production is the manufacturing of a novel kind of TiO_2 NPs and achievement its best antibacterial activity.

Key words: Antibacterial activity, Particle size, Sol-gel Method, $TiCl_3$, TiO_2 nanoparticles.

Introduction:

Titanium dioxide nanoparticles (TiO_2 NPs) have been of interest in a wide range of applications such as photocatalyst (1), a gas sensor (2), dye-sensitized solar cells (3), Nanomedicine (4), and antibacterial specialists (5). Acknowledged as an exemplary inorganic antibacterial biomaterial, TiO_2 NPs have been given much interest due to the strong and broad-spectrum antimicrobial action. Furthermore, TiO_2 NPs present good biocompatibility, excellent biosecurity, and exceptional hydrophilicity (6). TiO_2 NPs is broadly utilized as a self-sanitizing and self-purifying material in various utilizations (7). TiO_2 NPs have been affirmed by the "American Food and Drug Administration (FDA)" for utilizing human sustenance and aggravated in nourishment contact materials (8). Bacterial and fungicidal impacts of TiO_2 on Escherichia coli, Staphylococcus aureus, and Pseudomonas aeruginosa have been accounted for (9). The investigation on the microbiocidal impact of TiO_2 NPs was done with E. coli infections, microorganisms and organisms malignancy (10, 11). It was reported that E. coli was executed by contact with TiO_2 NPs. Hydroxyl radicals (•OH) and Responsive Oxygen Species (ROS) produced on the TiO_2 surface allow a section in inactivating microorganisms by oxidizing the polyunsaturated phospholipid part of the cell layer of organisms (6,9,12,13,14). TiO_2 NPs are around one thousand or conceivably ten thousand times more dynamic for E. coli inactivation than normal disinfectants, for instance, chlorine, ozone and chlorine dioxide (9, 12). There are three differing crystalline types of TiO_2 which are anatase, rutile, and brookite. Anatase and rutile have a crystalline structure that thinks about to the tetragonal framework while brookite has an orthorhombic crystalline structure (15, 16). The rutile structure is a thermodynamically stable stage everywhere

[1]Department of Physics, College of Science, Wasit University, Wasit, Iraq.
[2]Minstry of Science and Technology, Baghdad, Iraq.
[3]Department of Biology, College of Science, Wasit University, Wasit, Iraq.
[*]Corresponding author: physicsali11@yahoo.com

temperature. Just anatase and rutile stages are of mechanical significance. In the two structures, the titanium molecule is encompassed by six oxygen particles and every oxygen iota are encompassed by three iotas of titanium (17). TiO_2 NPs have been synthesized using various techniques, for example, hydrothermal (18), sonochemical (19), solvothermal (20), Reverse micelle (21), and sol-gel method (22) for those applications. As of late, the sol-gel process has been utilized for the planning of TiO_2 NPs (23). Exploratory outcomes have demonstrated that this technique had effectively delivered uniform size, un agglomerated state, high immaculateness and homogeneous nanoparticles (24). In this study, firstly we will synthesis TiO_2 NPs by using the sol-gel method and study the structural properties of TiO_2 NPs by X-ray diffraction, Atomic Force Microscopy, and transmission electron microscopy. Finally, the antibacterial activity of the prepared TiO_2 NPs will be studied.

Materials and Methods:

Preparation of TiO_2 Nanoparticles

Nanoparticles TiO_2 were prepared by using a sol-gel method. Titanium tetrachloride ($TiCl_3$) (99.9%, Sigma–Aldrich), and ammonium hydroxide (NH_4OH) (98%, Sigma– Aldrich) were utilized as the titanium antecedent. 50 ml $TiCl_3$ solution was slowly added dropwise to 150 ml NH_4OH for 1h. The reaction was performed at 50℃ under enthusiastic mixing at 700 rpm for 2hrs, creating the last arrangement. At first, the mixture is black and then becomes violet, after that it changes to deep blue like a clear sky and then gradually turns to the white homogeneous solution. The pH of the resulting solution is measured and adjusting to the value 3 by using hydrochloric acid (HCl, 37%, ROMIL). The solution was transformed into a gel by using ultrasonic bath device for 2hrs. At long last, the gel was thoroughly washed with refined water a few times for evacuating the polluting influences (alkali and chlorine ions). The gel was dried at 70˚C for 24hrs, the last powders were calcined at various temperatures 500˚C and 700˚C for 1h in an ambient atmosphere, the powder transforms to TiO_2 NPs in anatase phase. The resulting powders were squeezed as tablets with a diameter 10 mm.

Preparation of Bacteria for the Sensitivity Test

Three types of bacteria were subcultured, Gram positive Staphylococcus aureus, Gram negative Pseudomonas aeruginosa, and Gram negative Escherichia coli. The bacterial was subcultured on a rich medium like tryptic soy agar to activate it and it was incubated at 37℃ overnight for the sensitivity test. The bacteria was suspended in physiological saline 0.85% and the turbidity of the suspension was compared with 0.5 McFarland turbidity standard tube which was equal to (1×10^8 Colony Forming Unit /ml), McFarland was prepared according to MacFaddin (2000): 0.05 mL of 1.17% barium chloride dehydrate ($BaCl_2$-$2H_2O$), with 9.95 mL of 1% sulphuric acid (H_2SO_4). 5mL was a liquated into screw-capped tubes of the same size which were used in the procedure, the standard was stored in dark at room temperature and was vortexed prior to use. The bacterial suspension swabbed on the surface of Muller Hinton agar (the general media used for antimicrobial sensitivity test). The TiO_2 NPs were placed on the surface of the agar using sterile forceps, this method termed the disc diffusion method and the dishes were incubated at 37 ℃ overnight from 18 to 24 hrs. then the inhibition zone was measured in mm.

Characterization

The crystalline structure of TiO_2 powder was examined by X-ray diffraction device model "Shimadzu-6000 XRD" which records the intensity as a function of Bragg's angle, with the following Stipulations: the target is copper with wavelength (λ=1.54060 °A), current (30mA) and voltage (40 kV). The scanning angle 2Θ (change) in the range of (10-70) degree with a velocity of (5 deg/min). The morphological surface analysis was carried out employing an atomic force microscope (SPM Ntegra NT – MDT). The SEM measurements are performed with a TESCAN VEGA 3.

Results and Discussion:

Structure Analysis

Powder X-Ray Diffraction (XRD) was utilized for characterization of the particles nanocrystalline size, crystal structures, the volume of the unit cell, the density of the unit cell, and lattice parameter. Fig.1 shows (XRD) pattern of calcined TiO_2 nanopowders at calcination temperatures 500 ˚C and 700 ˚C. We named the predominant peaks linked with anatase (A) and rutile(R) phases. It can be seen that specimen showed the anatase TiO_2 crystal structure at a calcining temperature 500 ˚C. But an anatase-rutile mixed phase was noticed at 700 ˚C. This is supported by numerous publications in which anatase has been reported to act as a nucleation site for rutile formation and consonant with the findings of the researchers (25, 26), this also may explain the phase transformation onset temperature of 700 ˚C.

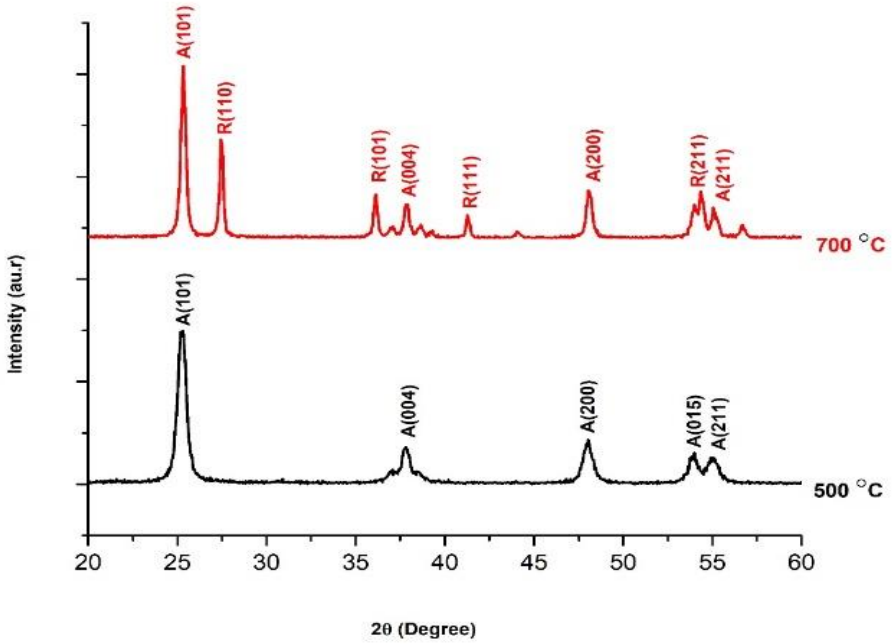

Figure 1. XRD patterns of TiO_2 powders synthesized at various calcination temperatures 500 ˚C, and 700 ˚C for 1h and pH 3 (A anatase and R rutile).

The XRD pattern showed that the sample calcined at 500 ˚C has three broad peaks 2Ɵ (change) angle at 25.289˚, 48.005˚, and 37.812˚ with (101), (200), and (004) diffraction planes, respectively. The XRD pattern showed that the sample calcined at 700 ˚C has three broad peaks 2Ɵ angle at 25.369˚, 27.501˚, and 54.372˚ with (101), (110), and (211) diffraction planes, respectively. The crystalline size of the prepared powders was calculated by using Debye–Scherer formula 1.

$$D = 0.9\,\lambda\,/\beta\cos\theta \quad \ldots\ldots\ldots\ldots\ldots\ldots\ldots\ldots 1$$

Where "D" is the crystallite size, "λ" is the X-ray wavelength, "β" is the full width at half maximum (FWHM), and "θ" is the diffraction angle (Bragg's angle) (7). The distance between the crystalline levels was calculated by eq. 2.

$$n\lambda = 2d\sin\theta \ldots\ldots\ldots\ldots\ldots\ldots\ldots\ldots\ldots\ldots\ldots 2$$

Where "d" is the distance between atomic layers in a crystal, "λ" is the wavelength of the incident X-ray beam, "θ" is the diffraction angle (Bragg's angle), and "n" is an integer representing the order of the diffraction peak (27, 28, 29). The lattice constants (a, b and c) were determined from the lattice spacing of Anatase (200) and (004) peaks in accordance with the Bragg equation for the tetragonal lattice structure (a= b ≠ c) using eq. 3.

$$1/d^2 = (h^2 + k^2/a^2) + (l^2/c^2) = 4\sin^2\theta/\lambda^2 \ldots\ldots\ldots\ldots\ldots (3)$$

Where "d_{hkl}" is the spacing between the planes conformable to "Miller indices (hkl)" (29). The volume of the unit cell for the samples was determined by using the relation 4.

$$V = a^2 \times c \ldots\ldots\ldots\ldots\ldots\ldots\ldots\ldots\ldots 4$$

Where "V" is the unit cell volume in cm^3, "a", and "c" is the lattice parameters. The densities were calculated using the formula 5.

$$\rho = FW \times Z/V \times N_A \ldots\ldots\ldots\ldots\ldots 5$$

Where "ρ" is the density (g/cm^3), FW is the formula weight, (FW= 79.89 gm/mol), Z is the number of unit cells (for anatase Z =4), "V" is the unit cell volume in cm^3, and "N_A" is Avogadro constant in per mol (29, 30). (XRD) comes about demonstrated that when the calcination temperature increment from 500 °C to 700 °C, the lattice parameters were slightly decreased, the FWHM decreased, and the average crystalline size increased. This outcome was likewise in great concurred with the last report (31, 32). Table1 summarizes the structural properties of TiO_2 nanoparticles.

Table 1. Structural properties of TiO_2 NPs synthesized at various calcination temperatures 500 °C and 700 °C for 1h and pH 3

Sample Calcination Temperature (°C)	TiO_2 at (500 °C)			TiO_2 at (700 °C)		
2 θ	Strongest 3 peaks			Strongest 3 peaks		
(Deg.)	25.28	48.005	37.812	25.369	27.50	54.37
FWHM (Deg.)	0.588	0.6323	0.5458	0.3295	0.243	0.2754
hkl	(101)	(200)	(004)	(101)	(110)	(211)
phase		Anatase		Anatase	Rutile	
Crystalline size D (nm)	14.46	14.36	16.06	25.8	35.13	33.86
Average Crystalline size D_{av} (nm)		14.96			31.59	
d_{hkl} Std.(Å)	3.5172	1.8929	2.3768	3.5172	3.243	1.685
d_{hkl} Exp.(Å)	3.5188	1.8936	2.3773	3.5079	3.240	1.686
Lattice parameters a=b (Å)		3.7873			3.7840	
Lattice parameters c (Å)		9.5093			9.4881	
Unit cell volume V ($Å^3$)		136.397			135.856	
Density, ρ (g/cm^3)		3.89			3.906	
Entry. Cod		96-710-3590			96-710-3590	

The morphological characteristics of the obtained TiO_2 NPs were investigated by the high resolution scanning electron microscopy (SEM). Fig. 2(a,b) shows the surface morphology of the TiO_2 NPs at calcination temperatures 500 and 700˚C, these images reveal that the shape of the particles is influenced by the experimental conditions and varied from spherical to elongate. SEM micrographs of the microstructures of all samples were analyzed by IMAGE J PROCESSING analysis to obtain the average particle size of the samples. The result showed that the average particle sizes grow bigger from 101.600 nm to 117.031 nm as the calcining temperature increased from 500˚C to 700˚C. The agglomeration becomes higher as the calcination temperatures increase. It is observed that in the higher calcination temperatures, the larger particle size with high uniform morphology is obtained for the samples calcined at 500 ˚C and 700˚C. This result is consonant with the findings of the researchers (3, 5, 23).

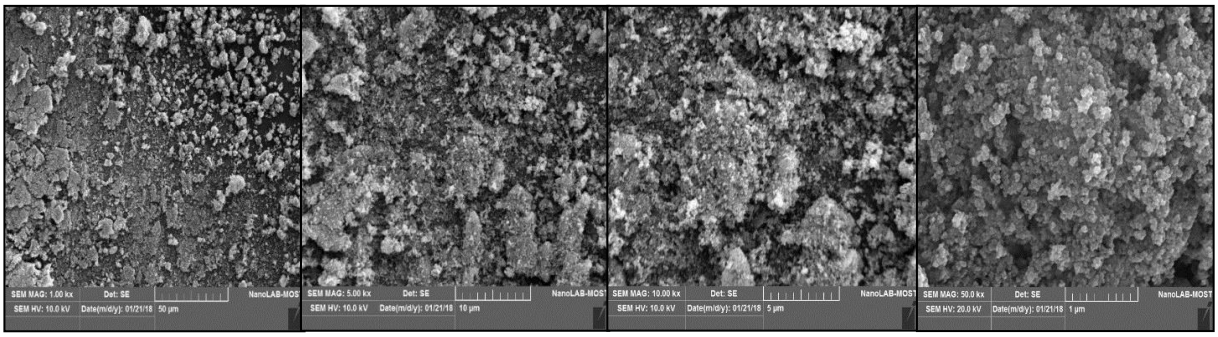

(a

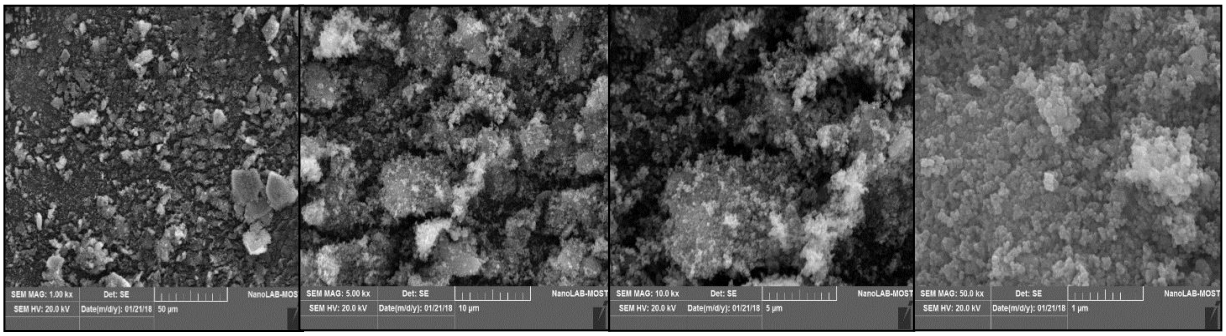

(b

Figure 2. SEM micrographs of TiO_2 NPs at pH3 with calcination temperature: (a) 500˚C and (b) 700˚C with four different magnifications 1.00kx, 5.00kx, 10.00kx and 50.00kx respectively (from the left to the right).

The topography, surface features, and the particle size of TiO_2 NPs were studied by using Atomic Force Microscope (AFM). Figure 3(a,b) shows the Atomic Force Microscope (AFM) three-dimension images and average grain size distribution in nanometer scale histogram for TiO_2 NPs with calcination temperatures 500 ˚C and 700˚C, it was found that the average grain size is 110 nm and 118.1 nm for the samples prepared at calcination temperatures 500 ˚C and 700˚C. The grain size increased as calcination temperatures increased from 500˚C to 700˚C. This result is consonant with the findings of the researcher (33).

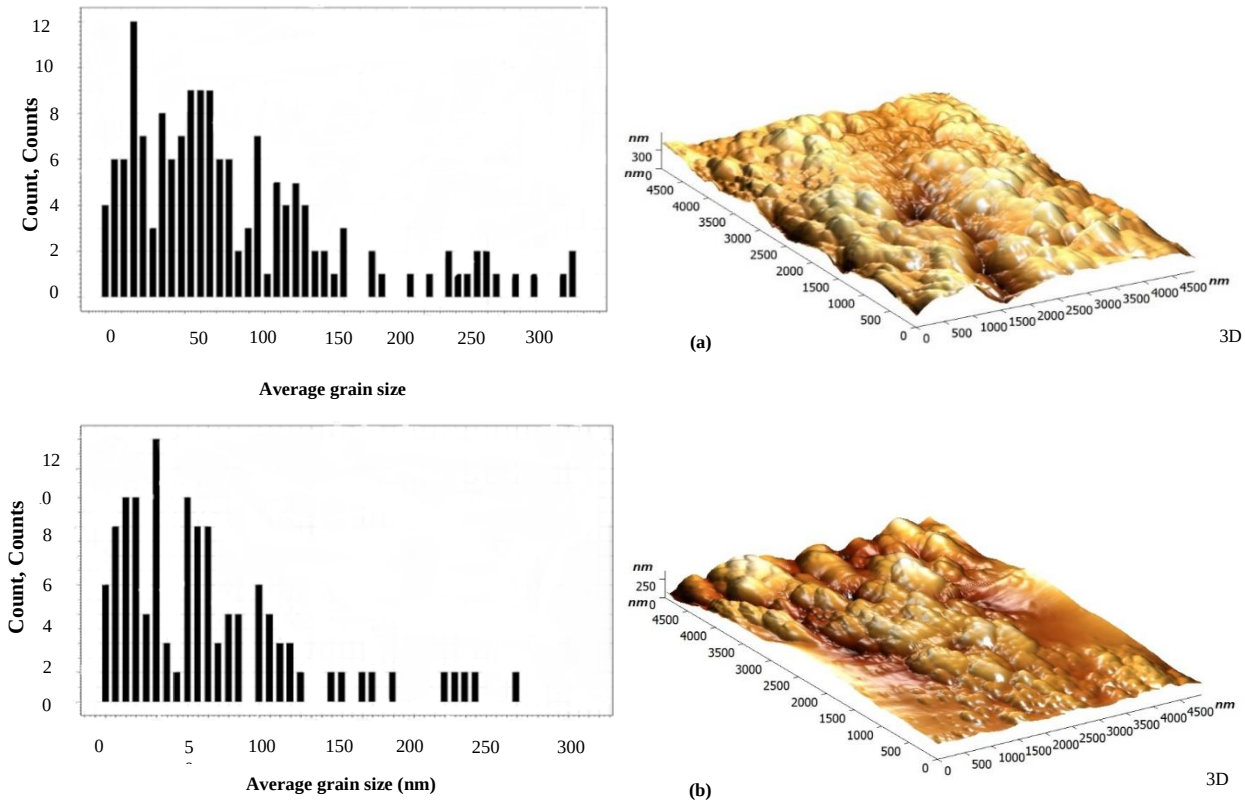

Figure 3. AFM 3D images and average grain size distribution in nanometer scale histogram at pH3 and calcination temperatures: (a) 500 ˚C, (b) 700 ˚C.

According to the characterization results of XRD, SEM, and AFM the particle size of TiO_2 NPs growth is related to the increment in the calcination temperatures. After calcination process crystalline size increase because OH links are broken and crystals start to grow, this result agrees with the findings of the researchers (23, 33). This might be because of the heat-initiated TiO_2 NPs accumulation and phase transmutation. The test discoveries deduced in this work are considered as better comprehension of the parameters that control the development of TiO_2 NPs while incorporating with the sol-gel technique. Likewise, the agglomeration becomes up higher when the temperature calcination is expanded. It is observed that in the higher calcination temperatures, a bigger particle size with irregular morphology was gotten for the samples calcined at high temperatures. An expansion of the temperature up to 700˚C, the size becomes up greater than 500˚C and the agglomeration end up critical. The particle size becomes greater as the calcining temperature was expanded to 700˚C, which clarified the impacts of warmth treatment on the particle size of TiO_2 NPs. Warm treatment is important to enhance the crystallinity of amorphous compounds. At the point when TiO_2 powders are calcined at a higher temperature, crystal structure changes may happen. The indistinct anatase and anatase-rutile advances depend firmly on the technique arrangements, the nature of the antecedent, and calcination conditions. Generally, the total change of amorphous to anatase has been observed to be finished at 500˚C, the anatase-rutile phase transformation has been done at 700 ˚C calcination temperature. The SEM pictures delineate that the greater part of the particles in spherical shape and impact of heat treatment on particle size was impressive. An expansion of

particle size with calcination temperature was expanded from 500 ˚C to 700˚C, ascribed to the crystal becomes bigger. The SEM and AFM result in great concurrence with XRD information estimated.

Antibacterial Activity of TiO_2 Nanoparticles

Results

According to the zone of restraint examination, Table 2 demonstrates the zone of bacteria development restraint for Staphylococcus aureus, E. coli, and Pseudomonas aeruginosa. The diameter of the inhibition zone was measured in mm. It was observed that when calcination temperatures of TiO_2 increase (increasing of TiO_2 NPs size), this leads to the decrease of the Zone of inhibition. The cause of increasing inhibition zone diameter was attributed to increasing the surface area of the reaction as the particle size of TiO_2 NPs decreased. The pictures of the zone of development restraint for Staphylococcus aureus, E. coli, and Pseudomonas aeruginosa appear in Fig. 4(a,b,c) The killing mechanism includes corruption of the cell surface and cytoplasmic layer because of the creation of Receptive Oxygen Species (ROS), for example, hydroxyl radicals and hydrogen peroxide. This at first leads to spillage of cell substance then cell lysis and might be trailed by total mineralization of the living being. Contact between the cells of the bacterium and TiO_2 NPs may influence layer porousness and this promptly expands harm to all cell divider layers, permitting spillage of little particles, for example, ions. Harm at this stage might be irreversible, and this goes with cell demise. Moreover, cell layer harm permits spillage of higher atomic weight parts, for example, proteins, which might be trailed by a bulge of the cytoplasmic layer into the encompassing medium through degraded zones of the peptidoglycan and lysis of the cell. Degradation of the inner parts of the cell at that point happens, then followed by entire mineralization. The degradation process may occur progressively from the side of the cell in contact with the TiO_2 NPs.

Table 2. Zone of microorganism's growth inhibition

Microbial Community	Zone of inhibition, the diameter of the zone (mm), TiO_2 NPs with pH3.	
	Calcination temperature (500℃)	Calcination temperature (700℃)
Staphylococcus aureus	43	41
E. coli	17	-
Pseudomonas aeruginosa	32	25

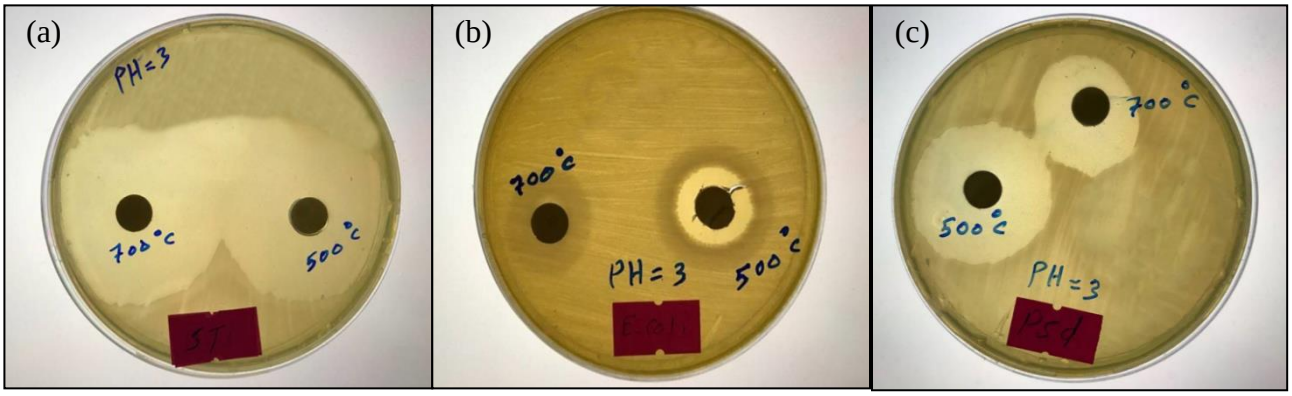

Figure 4. the antibacterial activity of TiO_2 NPs of different calcination temperature 500℃ and700℃ at pH 3 against (a) Staphylococcus aureus, (b) E. coli, (c) Pseudomonas aeruginosa.

Conclusion:

TiO_2 NPs were prepared by using the sol-gel method. The structure and morphology were characterized using different techniques XRD, SEM, and AFM. From XRD characterization, the sample calcined at 500℃ indicates Anatase phase with average crystallite size 14.96 nm and the sample calcined at 700℃ indicate Anatase-Rutile mixed phase with average crystallite size 31.59 nm. From the estimation of SEM and AFM, it is demonstrated that an expansion in particle size of TiO_2 NPs is related with the expansion in the calcination temperatures and the diameter of the inhibition zone. It is found that the average grain size of the sample calcined at 500℃ is 110 nm, and the average grain size of the sample calcined at 700℃ is 118.1 nm. It was observed that when calcination temperatures increased, the TiO_2 NPs size increased and the zone diameter of inhibition decreased. The results showed that TiO_2 NPs are a viable material for antibacterial agents of Gram positive Staphylococcus aureus, Gram negative Pseudomonas aeruginosa, and Gram negative Escherichia coli.

Conflicts of Interest: None.

References:

1. Veerachandra KY, Yen CH. Selection of photocatalytic bactericidal titanium dioxide (TiO_2) nanoparticles for food safety applications. LWT-Food Sci Technol. 2015 Apr; 61 (1):1-6.
2. Jing B, Baoxue Z. Titanium Dioxide Nanomaterials for Sensor Applications. Chem Rev. 2014 June; 114 (19): 10131-10176.
3. Kashyout AB, Soliman M, Fathy M. Effect of preparation parameters on the properties of TiO_2 nanoparticles for dye sensitized solar cells. Renew Energ. 2010 Dec; 35 (12):2914-2920.
4. Wang YQ, Zhang HM, Wang RH. Investigation of the interaction between colloidal TiO_2, and bovine hemoglobin using spectral method. Colloid Surface B. 2008 Sep; 65(2):190-196.
5. Yage X, Xihong L, Li Z, Qinglian X, Zhenming C, Weili L, et al. Effect of TiO_2 nanoparticles on the antibacterial and physical properties of polyethylene-based film. Prog Org Coat. 2011 Nov; 73 (2-3): 219–224.
6. Cijun S, Chenying S, Pei F, Chengde G, Shuping P, Youwen Y. Antibacterial Capability, Physicochemical Properties, and Biocompatibility of $nTiO_2$ Incorporated Polymeric Scaffolds. Polym. 2018 Mar; 10(3): 328-343.
7. Galkina OL, Sycheva A, Blagodatskiy A, Kaptay G, Katanaev VL, Seisenbaeva GA, et al. The sol–gel synthesis of cotton/TiO_2 composites and their antibacterial properties. Surf Coat Technol. 2014 Aug; 253:171-179.
8. Xiaojia H, Huey MH. Nanotechnology in food science: Functionality, applicability, and safety assessment. J Food Drug Anal. 2016 Jul; 24(4): 671-681.
9. Anna ZJ, Zhishun W, Izabela W, Piotr S, Ewa K. The effect of nanoparticles size on photocatalytic and antimicrobial properties of Ag-Pt/TiO_2 photocatalysts. Appl Surf Sci. 2015 October; 353: 317-325.
10. Shirajahammad MH, Vani RD, Delicia AB, Malatesh SP, Jagadish SK, Shyamkumar V, et al. Photocatalysis effect of a novel green synthesis gadolinium doped titanium dioxide nanoparticles on their biological activities. J Photochem Photobiol A. 2017 Sep; 346(1): 159-167.
11. Anila F, Tabeer K, Azra Y. Microbial synthesis of nanoparticles and their potential applications in biomedicine. J Appl Biomed. 2017 Nov; 15(4): 241-248.
12. Elnaz B, Alireza D, Nader H, Hadi V, Fatemeh SR. A study on Inhibitory Effects of Titanium Dioxide Nanoparticles and its Photocatalytic Type on Staphylococcus aureus, Escherichia coli and Aspergillus flavus. Appl Food Biotechnol. 2016 Jan; 3 (2):115-123.
13. Jiang W. Bacterial Toxicity of Oxide Nanoparticles and Their Effects on Bacterial Surface Biomolecules. PhD [dissertation]. United States: Boston. University of Massachusetts; 2011.
14. Siti HO, Nurul RAS, Norhazlizam Z, Roseliza KB, Rosnita AT. Antimicrobial Activity of TiO_2 Nanoparticle-Coated Film for Potential Food Packaging Applications. Int J Photo. 2014 Apr; 2014: 1-6.
15. Zebao R, Shangren W, Chao P, Hongbing J. Comparison of TiO_2 Degussa P25 with anatase and rutile crystalline phases for methane combustion. Chem Eng J. 2014 May; 243(1): 254-264.
16. Norman SA, Noredine M, Vladimir V, Peter JK, Roelof JK. The effect of crystalline phase (anatase, brookite and rutile) and size on the photocatalytic activity of calcined polymorphic titanium dioxide (TiO_2). Polym Degrad Stab. 2018 April; 150(1):31-36.
17. Ulrike D. The surface science of titanium dioxide. Surf Sci Rep. 2003 January; 48(5-8): 53-229.
18. Zhenquan T, Kazuyoshi S, Satoshi O. Synthesis of layered nanostructured TiO_2 by hydrothermal method. Adv Powd Technol. 2015 Jan; 26(1): 296-302.
19. Mizukoshi Y, Makise Y, Shuto T, Jinwei H, Tominaga A. Immobilization of noble metal nanoparticles on the surface of TiO_2 by the sonochemcal method: photocatalytic production of hydrogen from an aqueous solution of ethanol. Ultrason Sonochem. 2007 Mar; 14(3):387 -392.
20. Yuxi Z, Honghe Z, Gao L, Vincent SB. Synthesis and electrochemical studies of a layered spheric TiO_2 through low temperature solvothermal method. Electrochim Acta. 2009 June; 54(16): 4079-4083.
21. Ryoji I, Takayuki F, Masato H, Teruhisa O. Synthesis of nanosized TiO_2 particles in reverse micelle systems and their photocatalytic activity for degradation of toluene in gas phase. J Mol Catal A: Chem. 2006 Dec; 260(1-2): 247-254.
22. Nachit W, Touhtouh S, Ramzi Z, Zbair M, Eddiai A, Rguiti M, et al. Synthesis of nanosized TiO_2 powder by sol gel method at low temperature. Mol Cryst Liq Cryst, 2016 May; 627(1):170-175.
23. Roohollah A, Sousan R, Naghi PA, Amin JK, Mohammad A. A systematic Investigation of Expermental Condition on the Particle Size and Structure of TiO_2 nanoparticles Synthesized by a Sol-Gel Method. J Ceram Process Res. 2012 Jan; 13(2):164-169.
24. Sapizah R, ShahidanR, Ainon H. Inactivation of Escherichia coli under fluorescent lamp using TiO_2 nanoparticles synthesized via Sol Gel method. Sains Malays. 2012 Feb; 41(2): 219-224.
25. Ding XZ, Qi ZZ, He YZ. Effect of hydrolysis water on the preparation of nano-crystalline titania powders via a sol-gel process. J Mater Sci Lett. 1995 Jan 31; 14(1):21-2.
26. Penn RL, Banfield JF. Formation of rutile nuclei at anatase {112} twin interfaces and the phase transformation mechanism in nanocrystalline titania. Am Mineral. 1999 May 1; 84(5-6):871-6.
27. Bragg WH, Bragg WL. The Reflection of X-rays by Crystals. Proc R Soc Lond A. 1913 July; 88(605): 428-438.
28. Conrado A, Maria PG. Biomineralization and Biomaterials Fundamentals and Applications. 1st Ed.

Sawston, Cambridge, UK: Woodhead Publishing; 2016. 19 p.
29. Cullity BD, Stock SR. Elements of X-Ray Diffraction. 3rd Ed. USA: Pearson New International Edition; 2013.p50.
30. Shahid H, Maqsood A. Influence of sintering time on structural, magnetic and electrical properties of Si–Ca added Sr-hexa ferrites. J Magn Magn Mater. 2007 Apr; 316(1): 73-80.
31. Sharmila JS, Ramalingom S, Ravidhas C, Moses RA. Effect of Calcination Temperature on Titanium Oxide Nanocrystallites in the Anatase Phase Synthesized By Sol-Gel Route. J Appl Phys. 2017 Aug; 9(4):32-39.
32. Yadanar WM, Tun TM, Wint YL. The Effect of Heat Treatment on Phase Transformation and Morphology of Nano-Crystalline Titanium Dioxide (TiO_2). Int J Sci Technol. 2017 June; 6(6):293-299.
33. Todorovic M, Stetsovych O, Moreno C, Shimizu TK, Custance O, Pérez R. Pentacene/TiO_2 anatase hybrid interface study by scanning probe microscopy and first principles calculations. Acs Appl Mater Intef. 2018 Sep 5; 10(40):34718-26.

تحضير جسيمات ثنائي أكسيد التيتانيوم (تيتانيا) النانوية باستخدام طريقة صّل-جلّ واستخدامها في تطبيقات مضادات البكتيريا

علي عبدالله فياض[1] **عباس فاضل عيسى[1]** **شذى شمعون بطرس[2]** **زينة شاكر شلال[3]**

[1,] قسم الفيزياء، كلية العلوم، جامعة واسط، واسط، العراق.
[2] وزارة العلوم والتكنلوجيا، بغداد، العراق.
[3] قسم الأحياء، كلية العلوم، جامعة واسط، واسط، العراق.

الخلاصة:

في هذا البحث تم تحضير جسيمات ثنائي أكسيد التيتانيوم النانوية (TiO_2) باستخدام طريقة صّل-جلّ عند وسط حامضي (pH3). جسيمات ثنائي أكسيد التيتانيوم تم تحضيرها من ثلاثي كلوريد التيتانيوم ($TiCl_3$) وهيدروكسيد الامونيوم (NH_4OH) وبنسبة 3:1 عند درجة حرارة 50 درجة مئوية، الجلّ المحضر تم تجفيفه عند درجة حرارة 70 درجة مئوية وذلك للحصول على المسحوق النانوي. المسحوق الناتج من عملية التجفيف تم معاملته حراريا عند درجات حرارة 500 و 700 درجة مئوية . تم دراسة التركيب البلوري ومورفولوجيا السطح والحجم الحبيبي باستخدام جهاز حيود الاشعة السينية (X-ray) و مجهر القوة الذرية (AFM) والمجهر الإلكتروني الماسح (SEM). أظهرت النتائج تكون طور (Anatase) من ثنائي أكسيد التيتانيوم وبمعدل حجم حبيبي (110) نانومتر عند درجة حرارة 500 درجة مئوية. في حين اظهرت النتائج طور مخلوط من (Anatase-Rutile) من ثنائي أكسيد التيتانيوم وبمعدل حجم حبيبي 118.1 نانومتر عند درجة حرارة 700 درجة مئوية. تم دراسة الفعالية ضد البكتيريا باستخدام طريقة كيربي – باور (اختبار الحساسية بطريقة الانتشار). حيث أظهرت النتائج فعالية جيدة لجسيمات ثنائي أكسيد التيتانيوم والعمل على تثبيط بكتيريا زائفة زنجارية سالبة الغرام و البكتيريا الكروية العنقودية موجبة الغرام و إشريكية قولونية سالبة الغرام. أن حساسية البكتيريا لجسيمات ثنائي أكسيد التيتانيوم تعتمد وبشكل كبير على الشكل البلوري ، مساحة السطح ، المسامية ، حجم الجسيم ، وحالة الأكسدة. حيث ان جسيمات ثنائي أكسيد التيتانيوم ذات الحجم الحبيبي الصغير اظهرت فعالية عالية ضد البكتريا في حين أن جسيمات ثنائي أكسيد التيتانيوم ذات الحجم الحبيبي الاكبر اظهرت فعالية أقل. نستنتج من ذلك انه يمكن استعمال مادة ثنائي أكسيد التيتانيوم النانوية على قتل بعض انواع البكتيريا.

الكلمات المفتاحية: فعالية مضادات البكتيريا، الحجم الحبيبي، طريقة صّل-جلّ، ثلاثي كلوريد التيتانيوم، جسيمات ثنائي أكسيد التيتانيوم.